

## Overview

# Density functional calculations of NMR chemical shifts and ESR $g$ -tensors

Georg Schreckenbach<sup>1</sup>, Tom Ziegler<sup>2</sup>

<sup>1</sup>Theoretical Division, MS B268, Los Alamos National Laboratory, Los Alamos, NM 87545, USA

<sup>2</sup>Department of Chemistry, University of Calgary, Calgary, Alberta, Canada, T2N 1N4

Received: 24 October 1997 / Accepted: 19 December 1997

**Abstract.** An overview is given on recent advances of density functional theory (DFT) as applied to the calculation of nuclear magnetic resonance (NMR) chemical shifts and electron spin resonance (ESR)  $g$ -tensors. This is a new research area that has seen tremendous progress and success recently; we try to present some of these developments. DFT accounts for correlation effects efficiently. Therefore, it is the only first-principle method that can handle NMR calculations on large systems like transition-metal complexes. Relativistic effects become important for heavier element compounds; here we show how they can be accounted for. The ESR  $g$ -tensor is related conceptually to the NMR shielding, and results of  $g$ -tensor calculations are presented. DFT has been very successful in its application to magnetic properties, for metal complexes in particular. However, there are still certain shortcomings and limitations, e.g., in the exchange-correlation functional, that are discussed as well.

**Key words:** Density functional theory – Electron correlation – NMR chemical shifts – Electron spin resonance – Relativistic effects – Transition metal complexes

## 1 Introduction

The application of density functional theory (DFT) to nuclear magnetic resonance (NMR) and electron spin resonance (ESR) spectroscopies is a very new subject. For instance, a 1993 book on calculations of NMR shieldings [1] that summarized the state of the art at the time does not really mention DFT at all (except for a brief, “philosophical” discussion [2] about its possible merits). During the last five years, DFT-based NMR calculations have seen a rapid development that is perhaps best described with the word “explosion”. Indeed, in the short-time span since the publication of

the book [1], the method has already entered the standard repertoire of quantum chemistry [3]. The theoretical description of NMR chemical shifts based on the more traditional *ab initio* techniques has seen a tremendous development as well, and both comprehensive and technical [4] as well as more general reviews [5–12] are available. In the present overview, we will exclusively concentrate on DFT calculations of the NMR shielding (chemical shift) and the ESR  $g$ -tensor. Further, we intend to focus on aspects that are peculiar to DFT or are connected to our own work. With “peculiar” we mean both areas of remarkable success as well as aspects that surface only in DFT applications – contributions of the current density are an example of the second category. We hope to illustrate the remarkable scope of applications for which DFT is well suited. Indeed, DFT is currently the *only* first-principle method for the important field of NMR in (transition) metal complexes [13]. At the same time, we want to show areas that need further development.

The earliest DFT calculations of NMR chemical shifts were done some 10 years ago. These calculations [14–16] were not at the point of practical applicability – mainly due to the use of very small basis sets and of an inappropriate approximation to the exchange-correlation (XC) functional. Modern applications of DFT to the calculation of NMR chemical shifts have been pioneered by Malkin et al. [17–20] with their DFT-IGLO (individual gauge for localized orbitals) method and by Schreckenbach and Ziegler [21–25] who used the gauge including atomic orbitals (GIAO) approach. A number of other implementations, mostly based on the GIAO method, have been presented since [26–29]. One important feature of DFT [30–34] is the relative ease with which correlation effects can be included, thus allowing applications to large systems, e.g., metal complexes. DFT-NMR calculations on metal complexes include the work of Kaupp et al. [13, 35–43], Schreckenbach et al. [44], Ruiz-Morales et al. [45–48], Ehlers et al. [49], Bühl et al. [50–56], de Dios [57], Wagener and Frenking [58], Chan et al. [59–61], and Godbout and Oldfield [62]. Kaupp et al. [13] have reviewed computational NMR

Correspondence to: G. Schreckenbach

studies on transition-metal complexes. Another, equally important feature is the inclusion of relativistic effects that has, so far, been achieved for DFT only. (One exception is the ab initio based work of Ballard et al. [63], Nakatsuji et al. [64–66], and Takashima et al. [67]. These authors do not, however, incorporate gauge corrections into their NMR formulations, but instead attempt to use more complete basis sets to deal with the “gauge problem” of magnetic properties [6, 9], nor do they include correlation effects.) Relativistic effects become important for any chemical feature of heavy element compounds [68], and NMR and ESR are no exception. Kaupp et al. [35, 36] included scalar relativistic effects in DFT calculations of the chemical shift by employing relativistic effective core potentials (ECP). In this way, the chemical shift of light ligands can be calculated quite successfully while the NMR of the heavy nucleus proper remains inaccessible. They were further able to calculate spin-orbit effects by using finite perturbation theory [69–71]. Schreckenbach and Ziegler [24, 25] used a Pauli-type [72] relativistic Hamiltonian and the frozen-core approximation [22]. Their method allows for the determination of the chemical shift both at the ligand nuclei and at the heavy center proper, thus making the important field of multinuclear NMR [73] accessible to theoretical studies. An extension to include spin-orbit effects is in progress [74].

The equivalent of the chemical shift in ESR spectroscopy is the electronic  $g$ -tensor [75]. Compared with recent progress for the shielding, the calculation of the  $g$ -tensor from modern first-principle quantum mechanics is still in its infancy. It has been pioneered by Lushington and Grein [76–79] in the ab initio field, and by Schreckenbach and Ziegler [25, 80] based on DFT.

This overview is organized as follows. In Sect. 2, some aspects of the general theory for DFT and magnetic effects will be summarized. This will be followed by a more detailed discussion of requirements for the XC functional – a problem that is, on the one hand, peculiar to DFT methods but which has, on the other hand, not yet been solved completely. We shall discuss briefly what is known to date (Sect. 3). Necessarily, Sect. 3 is a more technical chapter, and a reader can easily skip over it. In Sect. 4, we will present the frozen-core approximation. It required disproving the common misconception that the chemical shift is a property of core molecular orbitals (MOs). We shall show that it is instead determined by the *core tail of valence MOs*. As an application, we will cite results of  $^{77}\text{Se}$  chemical shift calculations [44]. We will discuss DFT in comparison to various ab initio approaches, using the  $^{77}\text{Se}$  nucleus as a representative test case. The frozen-core approximation forms a basis for the inclusion of relativistic effects; NMR shielding calculations with relativity will be discussed in Sect. 5. We will utilize  $^{17}\text{O}$  NMR in transition-metal-oxo complexes  $\text{MO}_4^{n-}$  [24, 35, 43] and  $^{125}\text{Te}$  NMR [47] as representative examples. Section 6 is dedicated to ESR  $g$ -tensors. We conclude with a brief summary and outlook (Sect. 7).

## 2 General theory and theory of NMR shielding

We do not intend to present the complete theory of either DFT or ESR/NMR calculations at this point, as it

would go far beyond the scope of the current overview. Some aspects thereof are, however, appropriate as they facilitate the subsequent discussions. Good introductions to the theory of DFT can be found in textbooks [30], original papers [81, 82], and in reviews [31–34]. The general theory of NMR and ESR calculations has been discussed in reviews [5–7, 9, 10] and in numerous original papers (e.g., [17–28, 80, 83]). Finally, a good general introduction to various second-order effects can be found, e.g., in McWeeny’s textbook [84]. We will use atomic units in the following, unless stated otherwise. They are defined by  $\hbar = m = e = 4\pi\epsilon_0 = 1$ ; the speed of light,  $c$ , becomes  $c = 137.03599$  [85].

Properties like the NMR shielding and the ESR  $g$ -tensor can be expressed as static second derivatives of the total energy with respect to two perturbations [84]. Thus, two derivatives w.r.t. the magnetic field give the magnetizability (magnetic susceptibility) [86]; magnetic field and nuclear magnetic moment, NMR shielding; magnetic field and electronic spin, ESR  $g$ -tensor; two magnetic moments at different nuclei, NMR spin-spin coupling constants [87, 88], and so on. This approach yields a convenient general theoretical framework for the treatment of various, seemingly very different properties. We will not elaborate further at this point, although the approach has been widely employed. The interested reader may refer to the literature [20, 21, 25, 80, 83].

DFT is based on an exact expression for the total energy  $E$  of an  $n$ -electron system [81]

$$E = \sum_i^n \int d\vec{r} \Psi_i^* \left( \frac{p^2}{2} + V_N \right) \Psi_i + \frac{1}{2} \int d\vec{r}_1 d\vec{r}_2 \frac{\rho(\vec{r}_1)\rho(\vec{r}_2)}{|\vec{r}_1 - \vec{r}_2|} + E_{\text{XC}} . \quad (1)$$

In Eq. (1),  $\rho = \sum_i^n \Psi_i^* \Psi_i$  is the electronic density of the system, the  $\{\Psi_i\}$  form a set of  $n$  orthonormal one-electron functions,  $V_N$  is the external (nuclear) potential, and  $\vec{p}$  is the momentum operator. Hence, the first integral represents the kinetic and potential energy of a model system with the same density but without electron-electron interaction. The second term is the (Coulomb) interaction of the electron density with itself.  $E_{\text{XC}}$ , the XC energy, and  $E$  proper are functionals of the density. The exact functional form for  $E_{\text{XC}}$  is unknown (it is, in fact, *defined* through Eq. (1) [34]), and the evaluation of various approximations is at the center of any application of DFT. We will discuss XC functionals in Sect. 3. From Eq. (1), the Kohn-Sham (KS) equations are usually derived [30, 82]:

$$h_{\text{KS}} \Psi_i = \epsilon_i \Psi_i , \quad (2a)$$

$$h_{\text{KS}} = \frac{p^2}{2} + V_{\text{KS}} = \frac{p^2}{2} + V_N + \int d\vec{r}_2 \frac{\rho(\vec{r}_2)}{|\vec{r}_1 - \vec{r}_2|} + V_{\text{XC}} . \quad (2b)$$

The XC potential  $V_{\text{XC}}$  is the functional derivative of the XC energy  $E_{\text{XC}}$  with respect to the density,  $\rho$  [30]. The expressions in Eqs. (1) and (2) can be extended to open-shell systems [30], a case that is relevant for ESR (Sect. 6), or to include relativistic effects [89–95] (Sect. 5).

We will now introduce another extension, namely the inclusion of magnetic fields. This is, of course, central to the properties in this overview. The magnetic field,  $\vec{B}$ , is most conveniently introduced by means of the so-called minimal coupling [84]

$$\vec{p} \xrightarrow{\text{substitute}} \vec{p} + \vec{A}/c \quad (3)$$

where  $\vec{A}$  is the vector potential of the field. This is, however, not the whole story in DFT. Rather, the XC energy  $E_{\text{XC}}$  becomes a functional of the relativistic four-current density which translates in non-relativistic theory to the electron density,  $\rho$ , and the current density,  $\vec{j}$  [96–99],

$$E_{\text{XC}}[\rho] \xrightarrow{\text{substitute}} E_{\text{XC}}[\rho, \vec{j}] . \quad (4)$$

While it is already difficult to find a suitable model for the (field-free) XC functional  $E_{\text{XC}}[\rho]$ , no acceptable model for the additional current dependency (Eq. 4) has been found to date (Sect. 3).

Another fundamental difficulty that surfaces in any treatment of magnetic fields, be it in DFT or otherwise, is the so-called gauge problem. Its origin, implications, and possible remedies have been discussed in detail elsewhere [1, 5–7, 9], and we will only mention it here. For any given magnetic field, there is considerable freedom in the choice of gauge for the vector potential [84]. In particular, the actual vector potential depends on the (arbitrary) coordinate origin. Further, the vector potential, rather than the observable, the magnetic field, enters the quantum mechanical expressions through the minimal coupling of Eq. (3). Any expectation value, including NMR/ESR properties, can only depend on the values of observable quantities, and the gauge dependence should vanish exactly. This is, indeed, the case for exact solutions of, e.g., the KS equations (Eq. 2) where large (infinite) basis sets are used. For approximate solutions with smaller (finite) basis sets there is, however, a strong dependence on the choice of gauge [6]. Possibly the best solution to the gauge problem is to employ field-dependent GIAOs as basis functions [83, 100, 101]:

$$\chi_\alpha(\vec{B}, \vec{r}) = \exp\left[-\frac{i}{2c}(\vec{B} \times \vec{R}_\alpha) \cdot \vec{r}\right] \chi_\alpha(\vec{r}) \quad (5)$$

where  $\chi_\alpha(\vec{r})$  is the usual field-free basis function (atomic orbital, AO) that is centered at position  $\vec{R}_\alpha$  and  $\chi_\alpha(\vec{B}, \vec{r})$  is the corresponding GIAO. The field-dependent pre-factor (Eq. 5) ensures that only *differences* of position vectors appear in expectation values. This eliminates any origin-dependence, even for approximate MOs and finite basis sets. The equivalence of the GIAO and the simpler ‘‘common gauge’’ approaches to the NMR shielding has been shown for the complete basis set limit [25]. Attaching a field-dependent phase factor to individual AOs (Eq. 5) has been compared to ‘‘nucleus-attached’’ basis functions in geometry optimizations [83]. Moving the basis functions along with the atomic centers is general practice in quantum mechanics. Instead of the GIAO approach, it is also possible to assign similar exponential pre-factors to other entities, e.g., to localized MOs. This is the idea of the IGLO approach [7, 102,

103]. Certain integrals are easier to evaluate analytically in IGLO methods than in GIAO schemes. This difficulty has been resolved recently, either by techniques that were borrowed from geometry optimization procedures [83] or by employing numerical integration [21, 25]. In comparing IGLO and GIAO results, it has been shown that GIAO calculations converge faster with the basis-set size [60, 83, 104, 105], and we can conclude that the GIAO approach is probably the best method available for magnetic properties. From the GIAO formulation of Eq. (5), we can derive working equations for the NMR shielding tensor,  $\vec{\sigma}$ . The absolute shielding  $\sigma$  is related to the more familiar chemical shift  $\delta$  as follows:

$$\delta = \sigma_{\text{ref}} - \sigma \quad (6)$$

where  $\sigma_{\text{ref}}$  is the absolute shielding of the reference compound (e.g., tetramethylsilane, TMS, for  $^1\text{H}$ ,  $^{13}\text{C}$ , and  $^{29}\text{Si}$  NMR). Note the opposite sign between  $\delta$  and  $\sigma$ . The GIAO shielding tensor is given in DFT as [21, 25]:

$$\vec{\sigma} = \vec{\sigma}^p + \vec{\sigma}^d \quad (7)$$

where  $\vec{\sigma}$  has been split up into its diamagnetic and paramagnetic parts. This separation is in general not unique, because only the total shielding is an observable quantity. However, it has been defined uniquely for the GIAO method [5], and we obtain the st tensor component

$$\sigma_{\text{st}}^d = \sum_i^n n_i \left\{ \frac{1}{c^2} \left\langle \Psi_i \left| \sum_v^{2M} d_{vi} \frac{1}{2r_N^3} [\vec{r}_N \cdot \vec{r}_v \delta_{\text{st}} - r_{N_s} r_{v_s}] \chi_v \right. \right. \right. \\ \left. \left. \left. + \frac{1}{c} \sum_{\lambda, v}^{2M} d_{\lambda i} d_{vi} \left\langle \chi_\lambda \left| \left[ \frac{\vec{r}_v}{2} \times (\vec{R}_v - \vec{R}_\lambda) \right]_s h_t^{01} \right| \chi_v \right. \right. \right. \right\} , \quad (8)$$

$$\sigma_{\text{st}}^p = \sum_i^n n_i \sum_{\lambda, v}^{2M} d_{\lambda i} d_{vi} \left\langle \chi_\lambda \left| \frac{1}{2c} (\vec{R}_\lambda \times \vec{R}_v)_s h_t^{01} \right| \chi_v \right. \\ \left. + \sigma_{\text{st}}^{\text{p,oc-oc}} + \sigma_{\text{st}}^{\text{p,oc-vir}} \right. . \quad (9)$$

In Eqs. (8) and (9), the following notation is used: the MO  $\Psi_i$  with occupation  $n_i$  has been expanded into the set of  $2M$  AOs  $\{\chi_\beta\}$  with expansion coefficients  $\{d_{\beta i}\}$ ,  $\vec{r}_N$  is the electronic position operator relative to the nuclear magnetic moment, and the operator  $h_t^{01}$  is defined as

$$h_t^{01} = \frac{i}{c} \left[ \frac{\vec{r}_N}{r_N^3} \times \vec{p} \right]_t . \quad (10)$$

It follows from Eq. (8) that the diamagnetic shielding depends on the unperturbed, zero-order electron density only, as it is diagonal in the KS orbitals. However, the paramagnetic shielding (Eq. 9) is due to the magnetic density matrix, i.e., the density (matrix) under the influence of the magnetic field [22]. This density is taken to first order in the field only, and it is expanded into the occupied and virtual zero-order MOs, giving the following shielding contributions:

$$\sigma_{\text{st}}^{\text{p,oc-oc}} = \sum_{ij}^{\text{occ}} n_i S_{ij}^{1,s} \langle \Psi_i | h_t^{01} | \Psi_j \rangle \quad (11)$$

and

$$\sigma_{\text{st}}^{\text{p,oc-vir}} = 2 \sum_i^{\text{occ}} n_i \sum_a^{\text{vir}} u_{\text{ai}}^{1,s} \langle \Psi_i | h_i^{01} | \Psi_a \rangle. \quad (12)$$

The second term of Eq. (8) and the first term in Eq. (9) are numerically insignificant in most cases, and will not be discussed here. How to calculate the first-order occupied-occupied and occupied-virtual coefficients  $S_{ij}^{1,s}$  and  $u_{\text{ai}}^{1,s}$  has been discussed in detail in the literature [21–25, 106]. The GIAO approach lends itself readily to an analysis of the calculated shieldings, in terms of the occupied and virtual MOs of the molecule (Eqs. 11, 12) [21, 45–49]. This analysis constitutes a major advantage of the GIAO method; it is intrinsically impossible for other methods like IGLO-based schemes [7, 37, 38].

### 3 Experience with XC functionals and current DFT

Existing XC functionals can be roughly divided into three groups, local density approximations (LDAs) [107], generalized gradient approximations (GGAs) [108–111], and hybrid functionals that incorporate part of the exact Hartree-Fock (HF) exchange [34, 112]. In addition, efforts have been made [18–20, 26, 29] to model the current dependency in the XC functional [96–99], Eq. (4). To start with the latter, Lee et al. [26] have presented results of GIAO shielding calculations using the functional of Vignale and Rasolt [98]. Calculated GGA results with and without the additional current functional terms are given in Table 1. This table [26] shows that the contributions from the current density are small. They are certainly not sufficient to bring, e.g., the calculated  $^{19}\text{F}$  shielding in  $\text{F}_2$  close to experiment. Two opposite conclusions are possible. Either the current contributions are not very important at all, or the employed approximate local current density functional [98] is completely insufficient. Becke has proposed a gradient-corrected current-density functional [99] but no results are available yet. Malkin has, in a different way, pursued the second avenue by proposing an ad hoc, empirical correction to the paramagnetic shielding (Eqs. 9–12) to model the current contributions to the NMR shielding [18–20]. While this “coupled sum-over-states density functional perturbation theory (SOS-DFPT)”

approach is quite successful (e.g., the  $^{17}\text{O}$  shielding in the ozone, terminal oxygen, is  $-1290$ ,  $-1429$ ,  $-1230$  ppm from experiments, “uncoupled” DFT, and “coupled” DFT, respectively [19]), it lacks, to a certain degree, a theoretical justification (other than the mentioned success in some applications) [26, 28]. Hence, it does not necessarily allow conclusions about the importance of the current XC terms. Olsson and Cremer [29] have implemented Malkin’s method, but without using an auxiliary fit basis for the Coulomb and XC integrals of Eq. (1). (The density fit basis used by Malkin et al. [17–20] includes only  $s$ ,  $p$ , and  $d$  functions.) It is interesting to note that they obtain shielding values which are up to 16 ppm smaller than those of Malkin et al. [18–20], with an increasing tendency for increasing numbers of electrons, and they suggest modifying Malkin’s empirical correction term. We can conclude that the discussion about current DFT is all but settled.

To return to the (density-only) XC functionals, the general consensus is that the simple LDA is insufficient for chemical shifts [17–21, 26–28]. The differences between various GGAs seem to be minor; no general trend has emerged. Hybrid functionals have also been tested. They seem to be slightly more accurate than the GGAs for first-row compounds [27]. Kaupp et al. [43], in their study of  $^{17}\text{O}$  NMR in transition metal complexes  $\text{MO}_4^{2-}$ , found that hybrid functionals were *inferior* to GGAs in this example. Bühl applied hybrid DFT to the calculation of  $^{57}\text{Fe}$  and  $^{103}\text{Rh}$  chemical shifts [52], with quite a dramatic effect, e.g., for  $^{57}\text{Fe}$ , by correlating computed with experimental chemical shifts, he obtained linear regression lines with slopes of 0.65 (GGA) and 0.97 (hybrid), respectively, i.e., the hybrid functional is clearly *superior* in these cases. An extreme example is the  $^{57}\text{Fe}$  shift in ferrocene (657 ppm, GGA; 1525 ppm, hybrid; 1532 ppm, experiment). The reason for these effects is not entirely clear. Test calculations [115], using GGAs [108, 109] and a moderate basis set, show that the  $^{57}\text{Fe}$  NMR in ferrocene is determined by Fe-based MOs, namely the highest occupied molecular orbital (HOMO) ( $e_2''$ ; essentially Fe  $dx^2 - y^2$ ,  $dx_y$ ), HOMO-1 ( $a_{ij}$  Fe  $dx^2$ ), and lowest unoccupied molecular orbital (LUMO) ( $e_1'$ ; Fe  $dxz$ ,  $dyz$ ). The dominating MO couplings, Eq. (9), include the HOMO-1 to LUMO and, to a lesser degree,

**Table 1.** Current density contributions in the exchange-correlation (XC) functional (cf. Eq. 4) to calculated absolute shieldings in a few small molecules. All numbers are cited from Lee et al. [26]

Molecule/nucleus	Absolute shielding (ppm)		
	Calculated		Experiment
	Without current terms	Including current terms	
HF $^1\text{H}$	29.82	29.85	$28.5 \pm 0.2$
$^{19}\text{F}$	403.97	405.05	$410 \pm 6$
CO $^{13}\text{C}$	-15.35	-20.21	$3 \pm 0.9$
$^{17}\text{O}$	-77.14	-83.66	$-42.3 \pm 17.2^a$
$\text{N}_2$ $^{14}\text{N}$	-84.82	-90.43	$-61.6 \pm 0.2$
$\text{F}_2$ $^{19}\text{F}$	-271.70	-280.92	-232.8
$\text{H}_2\text{O}$ $^{17}\text{O}$	317.86	316.64	$344.0 \pm 17.2^a$
$\text{CH}_4$ $^{13}\text{C}$	184.33	182.92	198.7

<sup>a</sup> It has recently been proposed [113], based on very accurate calculations, to correct the experimental  $^{17}\text{O}$  absolute shielding scale [114] towards the lower error bar

the HOMO to LUMO transitions. We conclude, with the words of Kaupp et al. [43], that “the search for a ‘universal’ functional is still a challenge.”

#### 4 Frozen-core approximation: is the NMR chemical shift a core property?

It is a common assumption that the NMR chemical shift is a property of the core electronic density near the NMR active nucleus. The fact that the nuclear spin interacts with the electronic movement around the nucleus  $N$ , and that this interaction is inversely proportional to  $r_N^2$  (Eq. 10) is the basis for this assumption. In their attempt to use a relativistic Pauli-type Hamiltonian (Sect. 5) Schreckenbach and Ziegler have proposed calculating NMR shieldings using the frozen-core approximation [22]. This method would never work if the above assumption was true, because all core MOs are taken from atomic calculations, kept frozen in subsequent molecular calculations, and excluded from the summation over occupied MOs in Eqs. (11) and (12). Hence, the core electronic density is explicitly excluded from contributing to chemical shifts in any way other than through its constant atomic (diamagnetic) contribution (Eq. 8); it is not allowed to add to molecular effects in the chemical shift, by coupling with virtual MOs. The valence MOs are, however, orthogonalized against all core MOs; this ensures their correct asymptotic behavior near the nucleus. (Contrast this with the usual ECP methods [116, 117]: there, the respective valence MOs (pseudo-orbitals) are *chosen* such that they possess the wrong asymptotic behavior near the nucleus, by smoothing away the core wiggles.) The technical details of the frozen-core approximation have been discussed elsewhere [22, 25]. Schreckenbach and Ziegler [22] were able to conclude that it is a useful tool for shielding calculations – if the valence space is increased to contain at least the  $ns, np, (n-1)p, (n-1)d$  shells

where  $n$  is the number of the given period in the periodic table of elements. This is illustrated for a few small molecules in Table 2, where we list the terms in the paramagnetic shielding (Eq. 9) that would be neglected for different core levels. Again, a more detailed analysis has been given elsewhere [22]. It follows clearly that the relative chemical shift is a valence property, and not a core property. More precisely, it is mostly determined by the *core tail of the valence orbitals*, due to the mentioned  $r_N^{-2}$  dependence (Eq. 10).

So far, we have discussed the frozen-core approximation rather formally. We will change gear somewhat, and turn to “real” applications. The DFT-GIAO scheme, including the frozen-core approximation, has been applied to investigate  $^{77}\text{Se}$  NMR in a broad range of compounds [44]. The  $^{77}\text{Se}$  nucleus has been chosen for several reasons. First, relativistic effects (Sect. 5) are not yet relevant for  $^{77}\text{Se}$  chemical shifts. Second, a wealth of experimental data is available [118]. Third, there are also a number of high-level computational studies in the literature [19, 119–121], and this allowed for a detailed evaluation of the DFT-GIAO approach. Finally, an experimental absolute shielding scale has been proposed [122], again allowing for a rigorous test of theoretical methods. To start with the latter, the  $^{77}\text{Se}$  experimental absolute shielding scale turns out to be not particularly useful for test purposes. This is because it contains an estimated correction of 300 ppm for the relativistic contraction of the core electronic density, cf. Sect. 5. Consequently, all (non-relativistic) theoretical results are too small by about 300 ppm. We assume the relativistic correction to be much smaller than 300 ppm. Indeed, non-relativistic and relativistic calculations of the shielding in a neutral, spherically averaged Se atom (Se:  $2p$  core, double  $\zeta$  core/triple  $\zeta$  valence basis [44]; BP86 XC functional [108, 109]) yield 2997 and 3070 ppm, respectively, resulting in a relativistic correction of 73 ppm. Consequently, we propose correcting the experimental absolute shielding scale [122], by using

**Table 2.** Frozen-core approximation: neglected terms in the paramagnetic part of the absolute shielding, as obtained from all-electron calculations [22] (values in ppm)

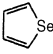
Molecule/nucleus	Absolute shielding		Paramagnetic part (Eq. 8)	Frozen-core level	Neglected terms <sup>a</sup>			
	Total	experiment			calculated	occ-occ <sup>b</sup>	occ-vir <sup>c</sup>	Total
C*O	3.0 ± 1.2; 1.0		-9.1	-264.0	1s	$\ll 10^{-3}$	-0.03	-0.03
Benzene (C)	57.2		52.6	-196.9	C: 1s	$\ll 10^{-3}$	-0.01	-0.01
	843		774.5	-279.0	C, O: 1s; S: 2s	$\ll 10^{-3}$	0.1	0.1
Cr*O <sub>4</sub> <sup>2-</sup>					S: 2p	4.4	4.0	8.4
		-2,384		-4,187	O: 1s, Cr: 2s	$\ll 0.1$	$\ll 0.01$	$\ll 0.1$
					Cr: 2p	6.2	18.2	24.4
					Cr: 3p	58.4	49.8	108.2
Te*F <sub>6</sub>					F: 1s, Te: 2p	-0.9	4.4	3.5
		2,256		-3,096	Te: 3p	9.8	10.3	22.1
					Te: 3d	10.4	15.2	25.6
					Te: 4p	14.6	14.2	28.8
					Te: 4d	425.1	-63.2	361.9

<sup>a</sup> Obtained from all electron calculations

<sup>b</sup> Core-core contributions to the occupied-occupied part of the paramagnetic shielding (cf. Eq. 11)

<sup>c</sup> Core-virtual contributions to the (leading) occupied-virtual part of the paramagnetic shielding (cf. Eq. 12)

**Table 3.** Calculated and experimental  $^{77}\text{Se}$  chemical shifts [44]. The experimental data refer to solution (s) or neat liquid (l), unless otherwise noted (g is for gas phase)

Molecule	Experimental $^{77}\text{Se}$ chemical shifts (ppm) <sup>a</sup>	Calculated $^{77}\text{Se}$ chemical shifts (ppm)				
		DFT-GIAO <sup>b</sup>	IGLO-HF <sup>c</sup>	GIAO-HF <sup>c</sup>	GIAO-MP2 <sup>c</sup>	GIAO-CCSD <sup>d</sup>
H <sub>2</sub> Se	-345 (g), -226 (s)	-425	-226	-270	-362	-335
(CH <sub>3</sub> )SeH	-155 (g), -116 (s)	-169	-118	-130	-180	
CH <sub>3</sub> CH <sub>2</sub> SeH	42	-17	16	11	-22	
Se(SiH <sub>3</sub> ) <sub>2</sub>	-666	-635	-657	-656	-700	
SeF <sub>4</sub>	1,083	1,174	922	966	1,175	
SeF <sub>6</sub>	631 (g), 610 (l)	714	551	577	727	
SeOF <sub>2</sub>	1,378	1,281	1,402	1,464	1,365	
SeO <sub>4</sub> <sup>2-</sup>	1,001–1,051	1034				
(CH <sub>3</sub> ) <sub>2</sub> C = Se	2,131 <sup>e</sup>	2,315	1,893	1,943	2,200	
Se = C = O	-447	-607	-368	-364	-532	-468
Se = C = Se	243(g), 331(l), 299(l)	222	402	446	121	281
	605	577	559	589	598	
Cyclic Se <sub>2</sub> <sup>2+</sup>	2,434 <sup>f</sup>	2,159 <sup>f</sup>		2,657 <sup>f</sup>	1,894 <sup>f</sup>	
Se <sub>4</sub> <sup>2+</sup>	1,923–1,958	1,834		3,821	154	

<sup>a</sup> Ref. [118]<sup>b</sup> Ref. [44]. The non-relativistic calculations have been carried out with a  $2p$  frozen core on Se, and a  $1s$  frozen core on O, C, N, and F<sup>c</sup> Refs. [119, 120]<sup>d</sup> Ref. [121]<sup>e</sup> Experimental result for <sup>t</sup>Bu<sub>2</sub>C = Se<sup>f</sup> Averaged over the distinct  $^{77}\text{Se}$  sites

a value of 70–75 ppm (instead of 300 ppm) for the relativistic correction.

Let us now return to the  $^{77}\text{Se}$  chemical shifts. Results from several methods, including DFT [44], HF [119, 120], second-order Møller-Plesset perturbation theory (MP2) [119, 120] and coupled-cluster singles-doubles (CCSD) [121] approaches are given in Table 3. The chemical shift of the reference compound, (CH<sub>3</sub>)<sub>2</sub>Se, has been set to zero, and has been omitted from the table. The calculated  $^{77}\text{Se}$  chemical shifts span a range of about 2800 ppm which includes almost the complete known experimental range [118]. Further, they cover a wide spectrum of bonding situations. Experimental gas-phase shifts are available for H<sub>2</sub>Se, (CH<sub>3</sub>)SeH, CSe<sub>2</sub>, and SeF<sub>6</sub> [118, 123]. Gas-phase data are desirable since such measurements come closest to the model situation underlying theory, isolated molecules without external interactions. (Gas-to-liquid shifts can be large indeed: e.g., 119 ppm for H<sub>2</sub>Se, Table 3.) We note from Table 3 that the DFT-GIAO method predicts the  $^{77}\text{Se}$  chemical shifts of these four compounds with higher accuracy than the GIAO-MP2 scheme; average errors between experiment and theory amount to 50 (DFT) and 65 ppm (MP2). The inferior performance of MP2 is due to its failure for the highly correlated CSe<sub>2</sub>, and MP2 is more accurate than DFT for the remaining three molecules. CCSD results are available for H<sub>2</sub>Se and CSe<sub>2</sub>. Errors are 10 and 38 ppm, respectively, making the GIAO-CCSD method superior to all other schemes mentioned. (The same is true when the individual tensor components of the shielding tensors are considered [44].) The small sample size prohibits a more detailed conclusion, and a larger set of data would have to be included for a more comprehensive judgment of the various methods.

So far, we have only discussed a few compounds. Considering also the rest of Table 3, we see that DFT performs well throughout. The same cannot be said about the ab initio methods. Both HF and MP2 fail for highly correlated molecules like CSe<sub>2</sub>, and, in particular, for the cyclic cations Se<sub>4</sub><sup>2+</sup> and Se<sub>3</sub>N<sub>2</sub><sup>+</sup>. Further, highly correlated ab initio methods that are known to give very accurate shieldings, like CCSD [121] (or even CCSD(T) [124]), are already beyond their limit for Se<sub>4</sub><sup>2+</sup>; they are too expensive computationally to be applicable to this ion. This illustrates a major advantage of DFT-based shielding calculations. While it has been disputed whether DFT is more accurate than MP2 for shieldings [12, 27–29, 44, 125–127], it is obvious that DFT can give a consistent picture, over a whole range of different bonding situations and, as we will see in the next section, throughout the whole periodic system. And this can be achieved at a very modest computational cost!

## 5 Relativistic NMR calculations

Taking only molecules at a given geometry into account (i.e., not considering the well-known relativistic bond contraction [68, 91]), there are three major mechanisms in which relativity influences NMR shieldings. First, relativity contracts the inner-core shells ( $s$  and  $p$ ). This leads to a contraction of the core electronic density which in turn yields a large increase in the diamagnetic shielding, as can be seen from Eq. (8). Since this is a core effect, it cancels out in relative chemical shifts (Eq. 6). Second, valence MOs are influenced by relativity as well, since they have to be orthogonal to the compact core MOs. Thus,  $s$ - and  $p$ -type orbitals are typically con-

tracted and stabilized, while  $d$  and  $f$  orbitals are more effectively screened from the nuclear charge, and are expanded and destabilized as a consequence [68]. These relativistic changes are reflected in the shieldings *and* the chemical shifts, primarily through the change in orbital energy differences: the strength of the magnetic interaction between different MOs is inversely proportional to their orbital energy differences [21, 22]. Third, spin-orbit interactions influence shieldings *and* chemical shifts [128]. Kaupp et al. [71] have presented a simple but general qualitative picture of the mechanism involved. The spin-orbit operators induce spin polarization in the system. This induced spin density interacts with the nuclear magnetic moment of the NMR-active nucleus, by means of a Fermi-contact mechanism – the same Fermi-contact term that is responsible for a large part of nuclear spin-spin coupling effects [87, 88].

Pyykkö [68] pointed out that the relativistic shielding tensor can be calculated either by third-order perturbation theory, or, similar to the non-relativistic case, Eqs. (7) to (12), by second-order perturbation theory, but then based on the relativistic MOs. Schreckenbach and Ziegler have followed the latter avenue. They have accounted for scalar relativistic effects, i.e., the first two relativistic effects, by using the so-called Pauli-Hamiltonian [72, 84]. In DFT, this requires inclusion in the KS equations (Eq. 2) of the mass-velocity operator,

$$h^{MV} = -p^4(8c^2) , \quad (13)$$

and the Darwin operator,

$$h^{Dar} = (1/8c^2)\nabla^2 V_{KS} . \quad (14)$$

To go beyond the scalar relativistic approach, one has to include Fermi-contact and spin-orbit operators as well [129]. The operators in Eqs. (13) and (14), possibly along with spin-orbit operators, are the foundation of the quasi-relativistic (QR) method of Snijders et al. [89–92], and they are also the basis for relativistic shielding calculations [24]. Details of the QR-NMR method have been given elsewhere [24, 25]. The QR method as outlined so far is not the only way to include relativistic effects in quantum chemistry [68]. We would like to mention one other approach, the use of relativistic ECPs [116, 117], still the most common relativistic method for structural chemistry and related problems. The use of ECPs for NMR calculations has been pioneered by

Kaupp et al. [35, 36]. As mentioned in Sect. 4, ECPs have, by construction, the wrong asymptotic behavior near the nucleus, making them unfit for NMR calculations at that center. ECPs are still useful for calculating the NMR at light, neighboring nuclei that can be treated without ECPs, and the results are comparable to calculated shieldings from the QR approach [24, 43].

Results of  $^{17}\text{O}$  calculations in transition-metal-oxo complexes  $\text{MO}_4^{n-}$  are summarized in Fig. 1 [24]. The agreement between theory and experimental data is good, although solvation shifts are expected to be important. The same systems have been studied by Kaupp et al. [35, 43] using their ECP-based DFT-IGLO scheme, and the two DFT methods agree to a reasonable degree [24, 43]. We note in passing that the method for localization of the MOs (which is not unique) can have a tremendous and unexpected influence on the calculated shieldings [43] – a problem that is inherent to the IGLO method but does not occur in the GIAO approach. Other applications of the QR-DFT-GIAO method include the proton NMR in transition-metal complexes [45], the  $^{13}\text{C}$ ,  $^{17}\text{O}$ , and metal NMR of carbonyl complexes  $\text{M}(\text{CO})_n$  [24, 46], and  $^{31}\text{P}$  chemical shifts in transition metal carbonyls [48]. In these studies, it has been possible to explain observed trends in the chemical shift based on the calculated electronic structure. The scalar relativistic DFT-GIAO method has also been applied to the NMR of heavy elements. An extensive investigation of  $^{125}\text{Te}$  chemical shifts has been performed [47], in continuation of the earlier  $^{77}\text{Se}$  NMR calculations [44] (Sect. 4). An experimental absolute shielding scale exists for the  $^{125}\text{Te}$  nucleus [122] but it is plagued by the same problem as the  $^{77}\text{Se}$  scale, namely, an estimated value for the relativistic contraction of the core density. Ruiz-Morales et al. [47] proposed correcting the experimental absolute shielding scale using more accurate values for the NMR of an isolated Te atom, in complete analogy to the discussion in Sect. 4. Calculated  $^{125}\text{Te}$  chemical shifts are summarized and compared to experimental data in Figs. 2–4. A detailed discussion of this data has been given elsewhere [47]. However, we would like to point out that DFT performs very well, with no exception, for the complete field of  $^{125}\text{Te}$  NMR. All this is achieved in a remarkably effective way, as illustrated by the size of some molecules. (The calculations have been performed at various workstations, i.e., without extraordinary computational resources.)

**Fig. 1.** Calculated and experimental  $^{17}\text{O}$  NMR shieldings in transition-metal-oxo complexes  $\text{MO}_4^{n-}$ ,  $\text{M} = \text{Cr}, \text{Mo}, \text{W}$  ( $n = 2$ );  $\text{Mn}, \text{Tc}, \text{Re}$  ( $n = 1$ );  $\text{Ru}, \text{Os}$  ( $n = 0$ ) [24]. The agreement between theory and experiment is satisfactory; remaining differences, for the  $3d$  complexes in particular, have been attributed [35] to shortcomings in the presently used exchange-correlation (XC) functionals. We note that relativity is crucial for a proper description of the  $4d$  and especially  $5d$  complexes

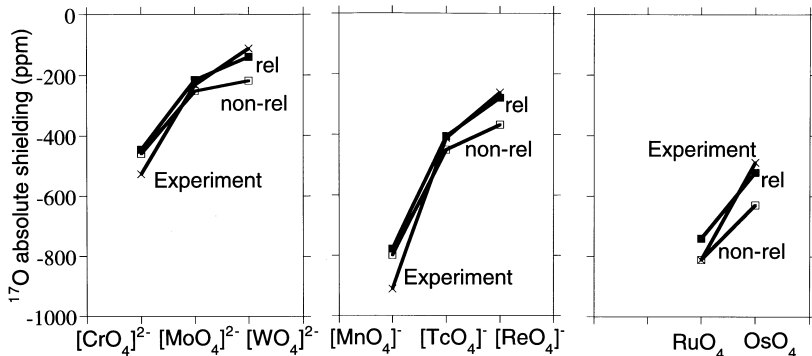


**Fig. 2.** Calculated and experimental  $^{125}\text{Te}$  chemical shifts of organic tellurium compounds [47]. The average deviation between theory and experiment is 235 ppm. The calculated chemical shifts span a range of 3000 ppm

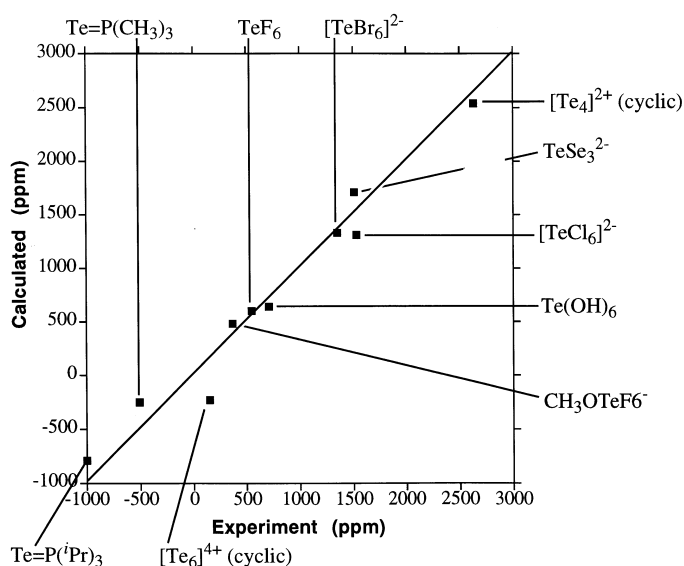
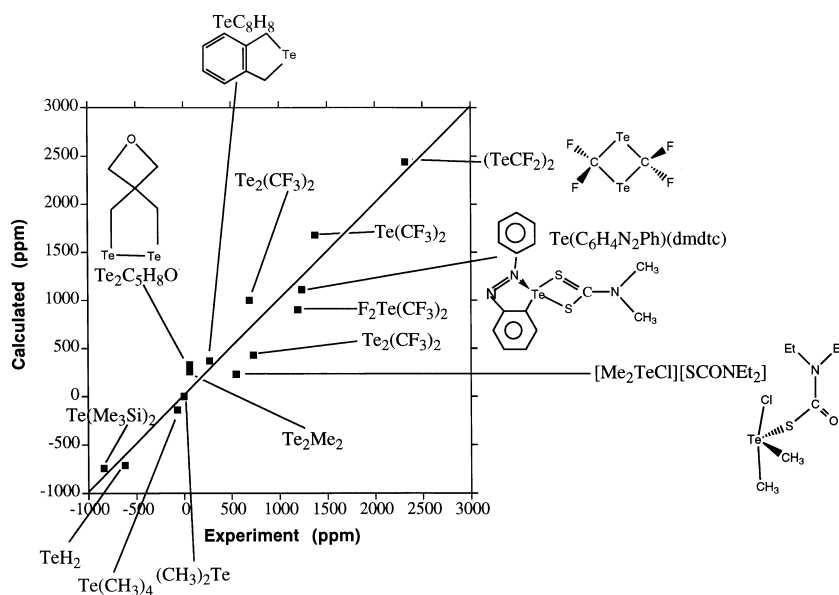


**Fig. 3.** Calculated and experimental  $^{125}\text{Te}$  chemical shifts of inorganic tellurium compounds [47]. The average deviation between theory and experiment is 160 ppm. The calculated chemical shifts span a range of 3400 ppm, thus covering almost the entire known shift range for the  $^{125}\text{Te}$  nucleus

At the end of this section, we have to mention certain shortcomings of the present QR approach. They are related to fundamental problems of the Pauli-Hamiltonian. The most severe problem seems to be that the mass-velocity operator of Eq. (14) has negative eigenvalues [130], which may lead to a variational collapse, i.e., to exceedingly large negative energies. This and related problems are circumvented in the QR approach by using the frozen-core approximation, thus treating only valence electrons variationally. The variational collapse is further avoided with a proper choice of valence basis functions, cf. the discussion by van Lenthe [95]. One such basis set requirement is that one must not

use more than a single  $\zeta$  core-type basis, which certainly influences the accuracy of calculated shieldings. These and other restrictions of the method have been discussed in detail [24]. None of them was found to prohibit quantitative agreement with experimental data.

## 6 ESR results

We will, in this section, leave the NMR shielding and discuss the ESR  $g$ -tensor. While the NMR shielding has seen tremendous theoretical activity recently, we have tried to discuss some of it in Sects. 3–5, nothing comparable has happened for the  $g$ -tensor yet.

ESR is based on the electronic Zeeman effect which is, for a free electron, described by the electron-spin Zeeman operator [75, 84]:

$$h_Z = \frac{g_e}{2c} \vec{S} \cdot \vec{B} . \quad (15)$$

In molecular systems, one can employ similar expressions, using an effective Zeeman interaction (e.g., for one unpaired electron) [131]:

$$h_Z^{\text{eff}} = \frac{1}{2c} \vec{S} \cdot \vec{g} \cdot \vec{B} . \quad (16)$$

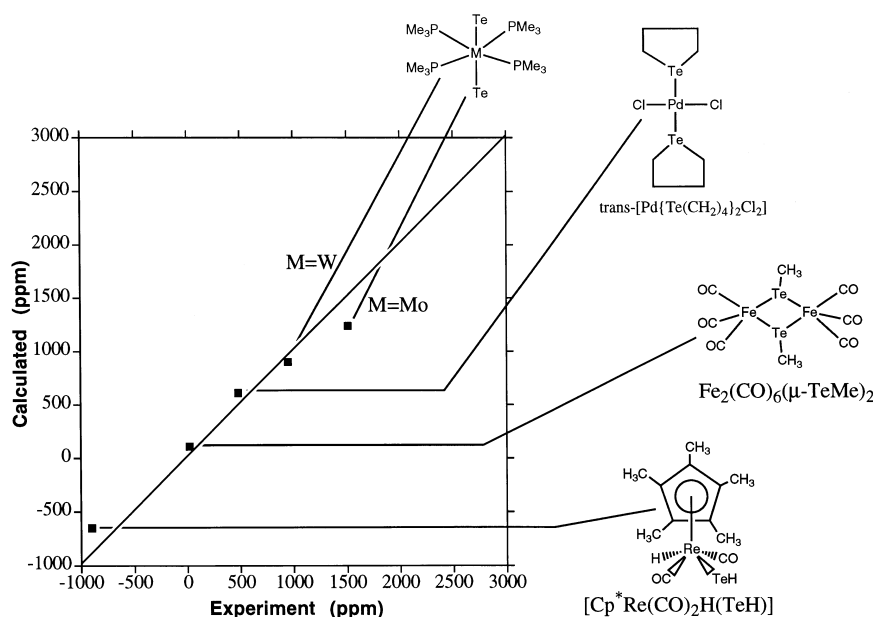
Equation (16) defines  $\vec{g}$ , the  $g$ -tensor, and  $\vec{S}$  is an effective spin operator. The effects of the molecular environment will be contained in the  $g$ -shift,  $\Delta g$ , that is defined as the deviation of the molecular  $g$ -value from the free electron value,  $g_e = 2.002319$  [75]:

$$\vec{g} = g_e \vec{1} + \Delta \vec{g} . \quad (17)$$

Note that, both  $\vec{g}$  and  $\Delta \vec{g}$  are second-rank tensors. Further,  $\vec{1}$  is the unit tensor, and  $\Delta g$  is the isotropic average of  $\Delta \vec{g}$ . According to Eqs. (15) and (16), only such operators contribute to  $\Delta \vec{g}$  that are either linear in the electronic spin, resulting in paramagnetic contributions (analogous to the paramagnetic NMR shielding of



**Fig. 4.** Calculated and experimental  $^{125}\text{Te}$  chemical shifts of organometallic tellurium compounds [47]. The average deviation between theory and experiment is 155 ppm. The calculated chemical shifts span a range of about 2400 ppm. Note the size of molecules that are accessible to DFT-NMR calculations. While relativistic effects are already important for  $^{125}\text{Te}$  in general [47], they are crucial for complexes of  $5d$  elements like tungsten



Eq. 9), or bilinear in the spin and magnetic field, giving diamagnetic contributions (cf. Eq. 8). Paramagnetic operators include the electron-nuclear spin-orbit operator, the electron-electron spin-orbit operator as well as the spin-other-orbit operator [75, 84]. Diamagnetic operators comprise a kinetic energy correction to the Zeeman operator of Eq. (15) as well as the diamagnetic contributions to the spin-orbit and spin-other-orbit operators; they are also called “gauge correction terms” in the literature [75].

First-principle DFT calculations of ESR  $g$ -tensor have been presented by Schreckenbach and Ziegler [25, 80], who recognized that the  $g$ -tensor can be formulated in almost complete analogy to the NMR shielding. That should not be too surprising from a theoretical point of view since, in either case, it is a spin magnetic moment that interacts with the external magnetic field, a nuclear spin for NMR, and an electronic spin for ESR. The analogy is fully exploited [80], and the sophisticated NMR apparatus can be used directly. We refer to the literature for further details of the theory [75, 80, 84, 131, 132]. The DFT-GIAO-ESR method has been tested for a variety of small radicals [80]. Some of the results are displayed in Figs. 5 and 6. The figures illustrate that theory is capable of reproducing experimental trends in both the isotropic molecular  $g$ -value (Fig. 5) and in its individual tensor components (Fig. 6). A detailed comparison with sophisticated ab initio methods [76–79] has been made [80]. The conclusion was that DFT results are in better agreement with experimental data than HF calculations; the best results are obtained by correlated multireference configuration interaction (MRCI) calculations. Similar trends have been observed in NMR shielding calculations [44] (Sect. 4). In Fig. 7, we demonstrate some of the difficulties that still exist when attempting to predict molecular  $g$ -values ( $g$ -shifts) theoretically. Thus, experimental numbers were in many cases obtained with the radical embedded in some host crystal. This makes the comparison of calculated and

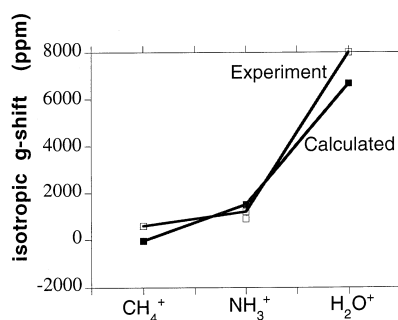


**Fig. 5.** Isotropic  $g$ -shift,  $\Delta g$ , in  $\text{CH}_4^+$ ,  $\text{NH}_3^+$ , and  $\text{H}_2\text{O}^+$  [80]

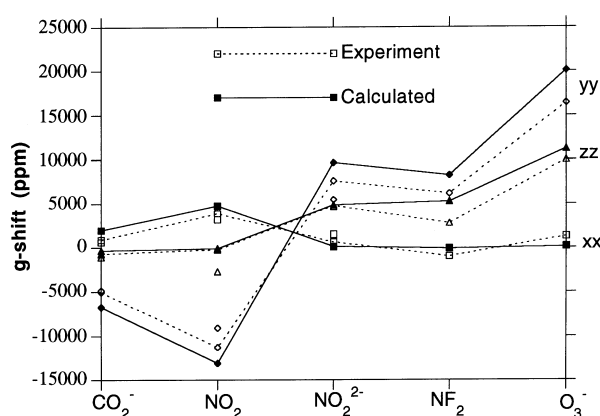


**Fig. 6.** Principal tensor components of the  $g$ -shift in symmetric  $\text{AB}_2$  radicals of first-row compounds [80]. The axis system was chosen such that the molecule lies in the  $yz$  plane, and that the  $z$  axis coincides with the twofold symmetry axis

experimental numbers difficult since the present calculations refer to the zero-pressure, zero-temperature limit of a gas-phase experiment. Experimental values can, on the other hand, vary considerably with the host crystal.

**Table 4.** Calculated and experimental isotropic  $g$ -shifts  $\Delta g$  for a few radicals (ppm). All numbers cited from Ref. [132]. Note that experimental numbers are generally given with two significant digits less

Molecule/ Component	Pauli operator		ZORA operator (spin-restricted)	Experiment	
	spin-unrestricted	spin-restricted			
NO <sub>2</sub>	$\Delta_{xx}$	4200	5000	5000	3900
	$\Delta_{yy}$	-13800	-16400	-16000	-11300
	$\Delta_{zz}$	-800	-600	-600	-300
HCO	$\Delta_{xx}$	2700	3200	3300	1400
	$\Delta_{yy}$	-300	-100	-200	0
	$\Delta_{zz}$	-9700	-12400	-12300	-7500
TiF <sub>3</sub>	$\Delta_{xx} = \Delta_{yy}$	-42800	-73300	-79700	-111300
	$\Delta_{zz}$	-1700	100	-1000	-11100
					-121500
				-11100	
				-123700	
				-3700	

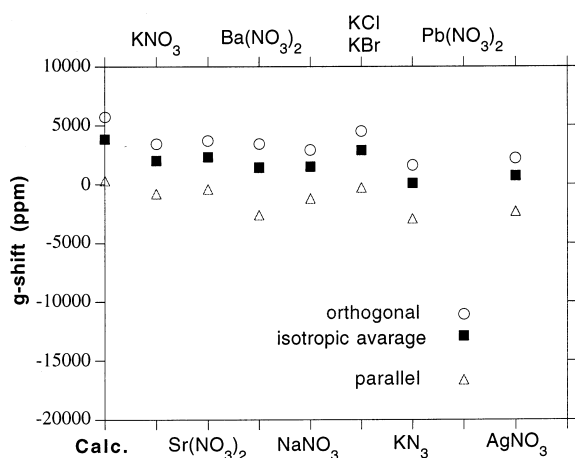


**Fig. 7.** Experimental  $g$ -shifts of the  $\text{NO}_3^-$  radical in different host crystals. The molecule possesses a threefold symmetry axis, and the principal tensor components of the  $g$ -shift correspond to coordinate axes that are parallel ( $\Delta g_{\parallel}$ ) and orthogonal ( $\Delta g_{\perp}$ ) to the symmetry axis. The figure illustrates the tremendous influence of the host matrix which can not yet be modeled by the current theoretical models

We see from Fig. 7 that the experimental range is enormous for our example  $\text{NO}_3^-$  [133]. To date, there is one other first-principle DFT implementation of the ESR  $g$ -tensor available. The work of van Lenthe et al. [132] is based on the “zero-order regular approximation for relativistic effects” (ZORA). ZORA [93–95] is a promising approach to relativistic quantum mechanics that avoids many of the shortcomings of the Pauli-Hamiltonian (cf. Sect. 5). We have collected results of van Lenthe et al. [132] in Table 4, where they are compared to our method [80]. Both methods give very similar results in spin-restricted calculations. Further, spin-unrestricted calculations turn out to be in better agreement with experimental values for  $\text{NO}_2$  and  $\text{HCO}$  while the spin-restricted approach is superior for  $\text{TiF}_3$ . Clearly, more data would be required for a comprehensive comparison of both methods.

Limitations of the DFT-ESR approach have been discussed [80], and they shall be mentioned now. The most severe limitation seems to be that the method fails for compounds of heavier nuclei. For example, the calculated parallel and orthogonal  $g$ -shift tensor components in  $\text{AlO}$  are  $-142$  and  $-222$  ppm while the

corresponding experimental values are  $-900$  and  $-2600$  ppm [80]. Schreckenbach and Ziegler attribute this to the perturbational treatment of the spin-orbit operator. Perturbation theory is expected to become increasingly inappropriate for heavier nuclei: relativistic effects are known to grow roughly with the square of the atomic number [68], and spin-orbit coupling is certainly a relativistic effect! Van Lenthe et al. [132] included the spin-orbit operators in all orders, and their method might be better suited for heavy elements.

## 7 Conclusion and future directions

We have tried to provide a feel for the progress that DFT calculations of magnetic properties have seen over the last few years. This development will, without doubt, continue. We see a number of directions for the development of DFT as applied to magnetic properties.

On the *fundamental side*, the discussion about appropriate XC functionals will certainly continue (Sect. 3). This includes, in particular, the search for useful approximations to the current dependency of the functional, or the proof that those contributions can be neglected! *Method development* and refinement will continue. We have discussed the success of approximate relativistic methods (Sect. 5). We have, however, also seen limitations that were either dictated by the use of ECPs at the heavy nucleus (Kaupp et al. [35]) or that are due to fundamental problems of the Pauli-Hamiltonian (Schreckenbach and Ziegler [24]). The problems of the latter approach can be tackled by replacing the, in a sense outdated, Pauli operator with a better relativistic method like the ZORA-Hamiltonian of van Lenthe [93–95]. Another, unrelated field where we foresee rapid development is the new idea of *linear scaling* methods. It will soon extend to second-order properties, including the ones discussed in this overview [134]. This is particularly important as current methods scale with, say, the third or fourth power of the system size. Linear scaling methods will open completely new areas for research. Further, *medium effects* of either solvents or solids should be accounted for (cf. Sects. 4 and 6). A promising first step in this direction has recently appeared in the literature [135, 136]. *Applications*, in particular to metal complexes, will undoubtedly continue. This is an area where theory can, quite successfully, guide the experi-

ment: e.g., the chemical shift range of metallic nuclei is generally large, often several thousand ppm, and it is a very cumbersome experimental task to scan this whole range for a chemical-shift signal.

The theoretical determination of ESR  $g$ -tensors (Sect. 6) has not yet seen the same amount of development as the NMR chemical shift. Thus, a lot remains to be done, including further testing of existing DFT methods, and their expansion to include the whole periodic system. No less important will be an extension to systems with an effective spin different from  $1/2$  or with degenerate, partially filled MOs; both are common situations in transition metal complexes and elsewhere. Practical applications will certainly appear, e.g., aiming to understand how the electronic structure manifests itself in the  $g$ -tensor.

*Acknowledgements.* One of us (G.S.) acknowledges funding by the Laboratory Directed Research and Development program of the Los Alamos National Laboratory, operated by the University of California under contract to the US Department of Energy. T.Z. acknowledges a Canada Council Killam Research Fellowship as well as the National Science and Engineering Research Council of Canada (NSERC) for financial support. We are grateful to M. Kaupp, M. Bühl, E. van Lenthe, D. Cremer, and G. Frenking for providing preprints prior to publication. Thanks are due to Y. Ruiz-Morales who contributed to the present studies.

## References

- Tossell JA (ed) (1993) Nuclear magnetic shieldings and molecular structure, NATO ASI C386. Kluwer, Dordrecht
- Pulay P (1993) In: Ref. [1], p 539
- Foresman JB, Frisch AE (1996) Exploring chemistry with electronic structure methods, 2nd edn. Gaussian, Pittsburgh, Pa.
- Jameson CJ (1980–1996) In: Webb GA (ed) Specialist periodic reports on NMR, vol 8–24. Royal Society of Chemistry, London
- Fukui H (1987) *Magn Reson Rev* 11: 205
- Chesnut DB (1989) In: Webb GA (ed) Annual reports on NMR spectroscopy, vol 21. Academic Press, New York, p 51
- Kutzelnigg W, Fleischer U, Schindler M (1990) In: Diehl PS (ed) NMR – basic principles and progress, vol 23. Springer, Berlin Heidelberg New York, p 165
- Cremer D, Olsson L, Reichel F, Kraka E (1993) *Isr J Chem* 33: 369
- Chesnut DB (1994) In: Webb GA (ed) Annual reports on NMR spectroscopy, vol 29. Academic Press, New York, p 71
- Chesnut DB (1996) In: Libkowitz KB, Boyd DB (eds) Reviews in computational chemistry, vol 8. Verlag Chemie, New York, p 245
- Gauss J (1996) *Ber Bunsenges Phys Chem* 99: 1001
- de Dios AC (1996) *Prog Nucl Magn Reson Spectrosc* 29: 229
- Kaupp M, Malkina OL, Malkin VG (1998) In: Schleyer PRv (ed) Encyclopedia of computational chemistry, Wiley, New York (in print)
- Bieger W, Seifert G, Eschrig H, Großmann G (1985) *Chem Phys Lett* 115: 275
- Friedrich K, Seifert G, Großmann G (1990) *Z Phys D17*: 45
- Friedrich K (1990) PhD thesis, Technische Universität Dresden, Dresden, Germany (in German)
- Malkin VG, Malkina OL, Salahub DR (1993) *Chem Phys Lett* 204: 80
- Malkin VG, Malkina OL, Salahub DR (1993) *Chem Phys Lett* 204: 87
- Malkin VG, Malkina OL, Casida ME, Salahub DR (1994) *J Am Chem Soc* 116: 5898
- Malkin VG, Malkina OL, Erikson LA, Salahub DR (1995) In: Politzer P, Seminario JM (eds) Modern density functional theory: a tool for chemistry. Elsevier, Amsterdam, p 273
- Schreckenbach G, Ziegler T (1995) *J Phys Chem* 99: 606
- Schreckenbach G, Ziegler T (1996) *Int J Quantum Chem* 60: 753
- Schreckenbach G, Dickson RM, Ruiz-Morales Y, Ziegler T (1996) In: Laird BB, Ross RB, Ziegler T (eds) Chemical applications of density functional theory. ACS Symposium Series 629. American Chemical Society, Washington, D.C., p 328
- Schreckenbach G, Ziegler T (1997) *Int J Quantum Chem* 61: 899
- Schreckenbach G (1996) PhD thesis, University of Calgary, Alberta, Canada
- Lee AM, Handy NC, Colwell SM (1995) *J Chem Phys* 103: 10095
- Cheeseman JR, Trucks GW, Keith TA, Frisch MJ (1996) *J Chem Phys* 104: 5497
- Rauhut G, Puyear S, Wolinski K, Pulay P (1996) *J Phys Chem* 100: 6310
- Olsson L, Cremer D (1996) *J Chem Phys* 105: 8995
- Parr RG, Yang W (1989) Density functional theory of atoms and molecules. Oxford University Press, New York
- Ziegler T (1991) *Chem Rev* 91: 651
- Ziegler T (1995) *Can J Chem* 73: 743
- Bartolotti LJ, Flurchick K (1995) In: Libkowitz KB, Boyd DB (eds) Reviews in computational chemistry, vol 7. Verlag Chemie, New York, p 187
- Becke AD (1995) In: Yarkony DR (ed) Modern electronic structure theory, part II. World Scientific, Singapore, p 1022
- Kaupp M, Malkin VG, Malkina OL, Salahub DR (1995) *J Am Chem Soc* 117: 1851
- Kaupp M, Malkin VG, Malkina OL, Salahub DR (1995) *Chem Phys Lett* 235: 382
- Kaupp M, Malkin VG, Malkina OL, Salahub DR (1996) *Chem Eur J* 2: 24
- Kaupp M (1996) *Chem Eur J* 2: 348
- Kaupp M (1996) *Chem Ber* 129: 527
- Kaupp M (1996) *Chem Ber* 129: 535
- Kaupp M (1996) *Chem Comm* 1141
- Kaupp M (1996) *J Am Chem Soc* 118: 3018
- Kaupp M, Malkina OL, Malkin VG (1997) *J Chem Phys* 106: 9201
- Schreckenbach G, Ruiz-Morales Y, Ziegler T (1996) *J Chem Phys* 104: 8605
- Ruiz-Morales Y, Schreckenbach G, Ziegler T (1996) *Organometallics* 15: 3920
- Ruiz-Morales Y, Schreckenbach G, Ziegler T (1996) *J Phys Chem* 100: 3359
- Ruiz-Morales Y, Schreckenbach G, Ziegler T (1997) *J Phys Chem A* 101: 4121
- Ruiz-Morales Y, Ziegler T (1997) *J Phys Chem A* (submitted)
- Ehlers AW, Ruiz-Morales Y, Baerends EJ, Ziegler T (1997) *Inorg Chem* 36: 5031
- Bühl M, Brintzinger H-H, Hopp G (1996) *Organometallics* 15: 778
- Bühl M, Malkin VG, Malkina OL (1996) *Helv Chim Acta* 79: 742
- Bühl M (1997) *Chem Phys Lett* 267: 251
- Bühl M (1997) *Organometallics* 16: 261
- Bühl M (1997) *J Phys Chem A* 101: 2514
- Bühl M, Hamprecht FA (1998) *J Comput Chem* 19: 113
- Bühl M (1998) *Angew Chem Int Ed Engl* 37: 142
- de Dios AC (1996) *Magn Reson Chem* 34: 773
- Wagener T, Frenking G, Inorg Chem (submitted)
- Chan JCC, Au-Yeung SCF, Wilson PJ, Webb GA (1996) *J Mol Struct (Theochem)* 365: 125

60. Chan JCC, Au-Yeung SCF (1997) *J Mol Struct (Theochem)* 393: 93
61. Chan JCC, Au-Yeung SCF (1997) *J Phys Chem A* 101: 3637
62. Godbout N, Oldfield E (1997) *J Am Chem Soc* 119: 8065
63. Ballard CC, Hada M, Nakatsuji H (1995) *Chem Phys Lett* 254: 170
64. Nakatsuji H, Takashima H, Hada M (1995) *Chem Phys Lett* 233: 95
65. Nakatsuji H, Nakajima T, Hada M, Takashima H, Tanaka S (1995) *Chem Phys Lett* 247: 418
66. Nakatsuji H, Hada M, Tejima T, Nakajima T, Sugimoto M (1995) *Chem Phys Lett* 249: 284
67. Takashima H, Hada M, Nakatsuji H (1995) *Chem Phys Lett* 235: 13
68. Pyykkö P (1988) *Chem Rev* 88: 563
69. Malkin VG, Malkina OL, Salahub DR (1996) *Chem Phys Lett* 261: 335
70. Kaupp M, Malkina OL, Malkin VG (1997) *Chem Phys Lett* 265: 55
71. Kaupp M, Malkina OL, Malkin VG, Pyykkö P (1998) *Chem Eur J* 4: 118
72. Pauli W (1927) *Z Phys* 43: 601
73. Mason J (ed) (1987) *Multinuclear NMR*. Plenum Press, New York
74. Wolff SK, Ziegler T, Schreckenbach G (1997) Spin-orbit and Fermi-contact in a DFT calculation of NMR shielding tensors. Poster presentation at the 3rd Canadian Computational Chemistry Conference, Edmonton, Alberta, Canada
75. Harriman JE (1978) *Theoretical foundations of electron spin resonance*. Academic Press, New York
76. Lushington GH, Bündgen P, Grein F (1995) *Int J Quantum Chem* 55: 377
77. Lushington GH, Grein F (1996) *Int J Quantum Chem* 60: 467
78. Lushington GH, Grein F (1996) *Theor Chim Acta* 93: 259
79. Lushington GH, Grein F (1997) *J Chem Phys* 106: 3292
80. Schreckenbach G, Ziegler T (1997) *J Phys Chem A* 101: 3388
81. Hohenberg P, Kohn W (1964) *Phys Rev* 136: B864
82. Kohn W, Sham LJ (1965) *Phys Rev A* 140: 1133
83. Wolinski K, Hinton JF, Pulay P (1990) *J Am Chem Soc* 112: 8251
84. McWeeny R (1989) *Methods of molecular quantum mechanics*, 2nd edn. Academic Press, London, New York
85. Cohen RE, Taylor BN (1987) *Phys Today* 40: 11
86. Colwell SM, Handy NC (1994) *Chem Phys Lett* 217: 271
87. Malkin VG, Malkina OL, Salahub DR (1994) *Chem Phys Lett* 221: 91
88. Dickson RM, Ziegler T (1996) *J Phys Chem* 100: 5286
89. Snijders JG, Baerends EJ (1978) *Mol Phys* 36: 1789
90. Snijders JG, Baerends EJ, Ros P (1979) *Mol Phys* 38: 1909
91. Ziegler T, Snijders JG, Baerends EJ (1981) *J Chem Phys* 74: 1271
92. Ziegler T, Tschinke V, Baerends EJ, Snijders JG, Ravenek W (1989) *J Phys Chem* 93: 3050
93. van Lenthe E, van Leeuwen R, Baerends EJ (1996) *Int J Quantum Chem Symp* 57: 28
94. van Lenthe E, Snijders JG, Baerends EJ (1996) *J Chem Phys* 105: 6505
95. van Lenthe E (1996) PhD thesis, Free University, Amsterdam
96. Rajagopal AK, Callaway J (1973) *Phys Rev B* 7: 1912
97. Rajagopal AK (1978) *J Phys C* 11: L943
98. Vignale G, Rasolt M (1988) *Phys Rev B* 37: 10685
99. Becke AD (1996) *Can J Chem* 74: 995
100. London F (1937) *J Phys Radium* 8: 397
101. Ditchfield R (1974) *Mol Phys* 27: 789
102. Kutzelnigg W (1980) *Isr J Chem* 19: 193
103. Schindler M, Kutzelnigg W (1982) *J Chem Phys* 76: 1919
104. Ruud K, Helgaker T, Bak KL, Jørgensen P, Jensen HJA (1993) *J Chem Phys* 99: 3847
105. Ruud K, Helgaker T, Kobayashi R, Jørgensen P, Bak KL, Jensen HJA (1994) *J Chem Phys* 100: 8178
106. Pople JA, Krishnan R, Schlegel HB, Binkley JS (1979) *Int J Quantum Chem Symp* 13: 225
107. Vosko SH, Wilk L, Nusair M (1980) *Can J Phys* 58: 1200
108. Becke AD (1988) *Phys Rev A* 38: 3098
109. Perdew J (1986) *Phys Rev B* 33: 8822
110. Lee C, Yang W, Parr RG (1988) *Phys Rev B* 37: 785
111. Perdew J, Wang Y (1992) *Phys Rev B* 45: 13244
112. Becke AD (1993) *J Chem Phys* 98: 5648
113. Sundholm D, Gauss J, Schäfer A (1996) *J Chem Phys* 105: 11051
114. Wasylshen RE, Mooibroek S, Macdonald JB (1984) *J Chem Phys* 81: 1057
115. Schreckenbach G (1997) (unpublished results)
116. Frenking G, Antes I, Böhme M, Dapprich S, Ehlers AW, Jonas V, Neuhaus A, Otto M, Stegmann R, Veldkamp A, Vyboishchikov SF (1996) In: Lipkowitz KB, Boyd DB (eds) *Reviews in computational chemistry*, vol 8. Verlag Chemie, New York, p 63
117. Cundari TR, Benson MT, Lutz ML, Sommerer SO (1996) In: Lipkowitz KB, Boyd DB (eds) *Reviews in computational chemistry*, vol 8. Verlag Chemie, New York, p 145
118. Duddeck H (1995) *Prog Nucl Magn Reson Spectrosc* 27: 1
119. Magyarfalvi G, Pulay P (1994) *Chem Phys Lett* 224: 280
120. Bühl M, Thiel W, Fleischer U, Kutzelnigg W (1995) *J Phys Chem* 99: 4000
121. Bühl M, Gauss J, Stanton JF (1995) *Chem Phys Lett* 241: 248
122. Jameson CJ, Jameson AK (1987) *Chem Phys Lett* 135: 254
123. Ellis PD, Odom JD, Lipton AS, Chen Q, Gulick JM (1993) In: Ref. [1], p 539
124. Gauss J, Stanton JF (1996) *J Chem Phys* 104: 2574
125. Facelli JC, Pugmire RJ, Grant DM (1996) *J Am Chem Soc* 118: 5488
126. Facelli JC, Orendt AM, Jiang YJ, Pugmire RJ, Grant DM (1996) *J Phys Chem* 100: 8286
127. Orendt AM, Facelli JC, Radziszewski JG, Horton WJ, Grant DM, Michl J (1996) *J Am Chem Soc* 118: 846
128. Pyykkö P, Görling A, Rösch N (1987) *Mol Phys* 61: 195
129. Cheremisin AA, Schastnev PV (1980) *J Magn Reson* 40: 459
130. Faradzel A, Smith VH Jr (1986) *Int J Quantum Chem* 29: 311
131. Abragam A, Bleaney B (1970) *Electron paramagnetic resonance of transition ions*. Clarendon, Oxford
132. van Lenthe E, Wormer PES, van der Avoird A (1997) *J Chem Phys* 107: 2488
133. Cunningham J (1968) In: Kaiser ET, Kevan L (eds) *Radical ions*. Wiley, New York, p 475
134. Ochsenfeld C, Head-Gordon M (1997) *Chem Phys Lett* 270: 399
135. Maurie F, Pfrommer BG, Louie SG (1996) *Phys Rev Lett* 77: 5300
136. Maurie F, Pfrommer BG, Louie SG (1997) *Phys Rev Lett* 79: 2340